Available online at www.sciencedirect.com
SCIENCE DIRECT®
Analytica Chimica Acta 549 (2005) 151–158
ANALYTICA CHIMICA ACTA
www.elsevier.com/locate/aca

# NIR spectrometry for counterfeit drug detection A feasibility study

Oxana Ye. Rodionova [a,*], Lars P. Houmøller [b], Alexey L. Pomerantsev [a], Paul Geladi [c], James Burger [c], Vladimir L. Dorofeyev [d], Alexander P. Arzamastsev [d]

[a] *Semenov Institute of Chemical Physics, Kosygin 4, 119991 Moscow, Russia*
[b] *Aalborg University Esbjerg, Denmark*
[c] *Unit of Biomass Technology and Chemistry, Swedish University of Agricultural Sciences, Umeå, Sweden*
[d] *Sechenov Moscow Medical Academy, Moscow, Russia*

Received 3 February 2005; received in revised form 6 June 2005; accepted 7 June 2005
Available online 11 July 2005

**Abstract**

Express-methods for detection of counterfeit drugs are of vital necessity. Visual control, dissociating tests or simple color reaction tests reveal only very rough forgeries. The feasibility of information-rich NIR-measurements as an analytical method together with multivariate calibration for mathematical data processing for false drugs detection is demonstrated. Also, multivariate hyperspectral image analysis is applied providing additional diagnostic information. Hyperspectral imaging is becoming a useful diagnostic tool for identifying non-homogeneous spatial regions of drug formulation. Two types of drugs are used to demonstrate the applicability of these approaches.


*Keywords:* Counterfeit drugs; Near infra-red spectrometry; Hyperspectral image analysis; Multivariate classification

## 1. Introduction

The problem of counterfeit drugs is important all over the world. For the first time the World Health Organization (WHO) obtained information about forgeries in 1982. At that time counterfeit drugs were mainly found in the developing countries. The definition for "counterfeit drug" by WHO is as follows: "A counterfeit medicine is one which is deliberately and fraudulently mislabeled with respect to identity and/or source. Counterfeiting can apply to both branded and generic products and counterfeit products may include products with the correct ingredients or with the wrong ingredients, without active ingredients, with insufficient active ingredient or with fake packaging" [1]. In the FIT conference in Sidney 2003 the definition was slightly changed: "Counterfeiting in relation to medicinal products means the deliberate and fraudulent mislabeling with respect to the identity, composition and/or source of a finished medicinal product, or ingredient for the preparation of a medicinal product" [2]. It was also mentioned that counterfeit may concern genuine drugs, generics, and traditional medicine.

Nowadays, the following types of fake drugs are encountered [3]:

1. Drugs that do not contain active substances including active substances marked in the packing, i.e. placebo (about 43%)
2. Drugs that contain active substances that are not marked in the packing (about 7%). Ordinary in such "medicine" the more expensive active substance is substituted by a less active and respectively cheaper substance. Also it is possible that drugs claimed to be "highly active medicine", for example a botanical medicine, really contain highly active substances, but they are steroid, ephedrine or their derived substances.

* Corresponding author. Tel.: +7 95 9397 483; fax: +7 95 9397 483.
*E-mail address:* rcs@chph.ras.ru (O.Ye. Rodionova).

0003-2670/$ – see front matter © 2005 Elsevier B.V. All rights reserved.
doi:10.1016/j.aca.2005.06.018

3. Drugs that actually contain the marked substance, but these drugs are produced by another manufacturer (about 50%). They include 21% with low content of active substance, about 5% improper packing, and about 24% with low quality drugs.

Nowadays, there are "high quality" counterfeit drugs that are very difficult to detect. It is worth mentioning that fake drugs include dietary supplements too. In such medicine non-declared substances such as hormones, ephedrine, etc., may be found.

According to WHO information [3] the spread of counterfeit drugs in different countries are as follows: 70% of turnover is in developing countries and 30% is in market-economy countries. The distribution of fake drugs with respect to different therapeutic groups is as follows: (1) antimicrobial drugs 28%; (2) hormone-containing drugs 22% (including 10% of steroids); (3) antihistamine medicines 17%; (4) vasodilators 7%; (5) drugs used for treatment of sexual disorders 5%; (6) anticonvulsants 2%; (7) others 19%. Visual control, disintegration tests or simple color reaction tests reveal only very rough forgeries [4–8]. More complicated chemical methods are also used [9–11] but all these methods try to prove or disprove the content and concentration of an active ingredient. But the main goal is to discriminate genuine and counterfeit drug, even in cases where the counterfeit drug contains the sufficient concentration of active ingredient and as a result to answer the question: "Does a given drug correspond to the original as it is marked on the package?" In many cases dosage forms contain not only active substances but also excipients. The exact content of excipients could differ for the genuine and fake drugs. In this paper, it is proposed to apply near infra-red (NIR) spectroscopy (14,000–4000 $cm^{-1}$) that could be used both for identification of pharmaceutical substances and dosage forms independently of contents of an active ingredient. NIR also could give information about the excipients in a pharmaceutical preparation and thereby be able to detect counterfeit drugs even with proper active substance.

Many different phenomena, not only chemical but also physical, have different individual contributions to the NIR spectra and this makes NIR measurements information-rich. Application of NIR spectrometry for investigations of different drugs has been performed before [12–14], but this approach is not used in pharmacopoeia practice as a routine procedure for counterfeit drug detection. It is known [15], that in the 1000–2500 nm (4500–9000 $cm^{-1}$) range, it is possible to shine light through several millimeters of material. This makes it possible for so-called diffuse reflectance, whereby light passing into a sample is scattered inside the sample and reflected back out and detected, carrying information about where it has been and what it has seen. That is why such detection is possible. On the other hand difference in coating also reveals forgery. However, NIR measurements are rapid, simple and also need no special sampling preparation. But these measurements carry information in a hidden way, and to extract the desirable information a special mathematical data processing is necessary.

A factor limiting significant advancement in these areas is that data obtained from such instruments are typically highly correlated and corrupted with noise, making it difficult to obtain the needed information. Multivariate data analysis (MDA) [15] assists in extracting the useful information. Examples of multivariate data analysis in pharmaceutical applications are comparatively few [16]. In this work, the well-known projection regularization methods principal component analysis (PCA) [17,18] and soft independent modeling of class analogy (SIMCA) [19] are applied.

## 2. Background

### 2.1. Principal component analysis

Data sets with many variables can be simplified by variable reduction and thereby be more easily interpreted. Principal component analysis (PCA) [18] is a well-known reduction technique:

$$\mathbf{X} = \mathbf{T}\mathbf{P}^{\mathrm{t}} + \mathbf{E} \tag{1}$$

where $\mathbf{X}$ is the $N \times K$ spectral data matrix, $\mathbf{T}$ the $N \times A$ matrix of score vectors, $\mathbf{P}$ the $K \times A$ matrix of loading vectors, $\mathbf{E}$ the $N \times K$ residual matrix, $N$ the number of objects, $K$ the number of variables (which in our case is the number of wavenumbers), and $A$ is the number of components calculated (i.e., principal components, PCs). $\mathbf{X}$ may be preprocessed by mean-centering or scaling. Vectors in $\mathbf{T}$ can be used to make score plots to present objects in a new space. Vectors in $\mathbf{P}$ can be used to make loading plots to show the inter-variable relationships. The number of components, $A$, is chosen with respect to the different criteria [15,18]. Among them are the eigenvalues $\lambda_a$ of the matrix $\mathbf{X}^{\mathrm{t}}\mathbf{X}$, and the standardized eigenvalues:

$$\mu_a = 100\frac{\lambda_a}{\mathrm{Tr}(\mathbf{X}^{\mathrm{t}}\mathbf{X})}, \quad a = 1, \ldots, A$$

where $\mathrm{Tr}(\mathbf{X}^{\mathrm{t}}\mathbf{X})$ is the trace of the matrix $\mathbf{X}^{\mathrm{t}}\mathbf{X}$.

### 2.2. Soft independent modeling of class analogy (SIMCA)

SIMCA is a supervised pattern recognition method [15,19]. The idea behind this method is that objects in one class or group show similar behavior and this approach allows the objects to display intrinsic individualities as well as their common patterns, but only common properties of the class are modeled [21]. Each group of objects is independently subjected to PCA and could be described by a different number of PCs. After that the distances between classes can be calculated and also the distance from a new object to the specified class can be calculated. In the present case, for the given type of drugs a class of genuine drugs is constructed and for each

new object $\mathbf{x}_i$ (which in this case is a spectrum) two distance measures can be calculated. The first is the object-to-model distance that is calculated as the residual standard deviation, $s_i$:

$$s_i = \sqrt{\frac{1}{K-A}\sum_{ij}\mathbf{e}_{ij}^2} \quad (2)$$

where $\mathbf{e}_i$ is the vector of residuals, i.e. $\mathbf{e}_i = \mathbf{x}_i - \mathbf{t}_i\mathbf{P}^t$, and $\mathbf{t}_i$ is a row vector containing the score values for sample no. $i$ on all principal components. $s_i$ is compared to the overall variation of the class, $s_0$:

$$s_0 = \sqrt{\frac{1}{(N-A-1)(K-A)}\sum_{ij}\mathbf{e}_{ij}^2} \quad (3)$$

and this is used for a statistical criterion ($F$-test) to decide whether a new sample can be classified as a member of the class or not. The second is the object-to-model-center distance calculated as the sample leverage:

$$h_i = \frac{1}{N} + \sum_{a=1}^{A}\frac{t_{ia}^2}{\mathbf{t}_a^t\mathbf{t}_a} \quad (4)$$

where $t_{ia}$ is the score value for sample no. $i$ on principal component no. $a$, and $\mathbf{t}_a$ is a column vector containing the score values for all samples on principal component no. $a$.

This measure shows how far the projection of a new object onto the model is from the class center.

### 2.3. Multivariate image analysis (MIA)

It is possible to extend PCA to multivariate images, providing the typical PCA score and loading vectors that can be used for interpretation of covariance structures. However, with Multivariate image analysis (MIA) the score vectors may additionally be re-arranged and viewed as score images. Score plots may be viewed to represent variance distributions from pairs of score vectors. Color intensity mappings may be additionally added to these score plots to help represent the relative intensities of individual score value parings [20]. These score plots may display clustering of pixels, outlier pixels and gradients. It is also possible to do interactive brushing between score plots and score images. The essence of MIA is the possibility to do interactive visual analysis. For example a pixel cluster in a score plot may be selected, with subsequent highlighting of the corresponding pixels in the score or raw images, or other score plots.

## 3. Experimental

Two types of drugs are analyzed. For both types measurements were made using a Bomem MB160 NIR spectrometer with "Powder Samplir" accessory for diffuse reflectance and two different detectors (InGaAs and InAs). For background spectrum, 50 (Data Set 1) or 100 (Data Set 2) scans of a "Spectralon" teflon disc were used, and for the samples 50 scans was used. The spectra are presented as log(1/reflectance) as a function of wavenumber. The explanation of the negative ordinate values seen in the spectra is that different gain settings were used for the background and the sample spectra respectively. No special sample preparation was used. Hyperspectal NIR images were acquired for the two drug tablets, using a Spectral Dimensions MatrixNIR camera. The matrixNIR can produce images of size 260 × 320 in up to 128 wavelengths in the range 900–1700 nm. Each tablet was crushed, carefully removing the tablet coating in the process. Small bottle caps were used to contain the powdered ingredients during imaging. For reasons of industrial confidentiality, no detailed information about chemical composition of the samples can be given.

### 3.1. Data Set 1: antimicrobial drug, film coated tablets, 250 mg

Two grades of film coated tablets containing drugs are investigated; grade "W" is a genuine drug and grade "Y" a counterfeit drug. Each grade is represented by three objects. Six different capsules are measured two times, one time from each surface, using the InGaAs detector. Thus, Data Set 1 contains 12 NIR spectra (4500–9000 $cm^{-1}$, 1169 wavenumbers).

Multiplicative scatter correction (MCS) [21] for each tablet grade was used as pre-treatment method. The correction coefficients are computed from a regression of each individual spectrum onto the average spectrum.

### 3.2. Data Set 2: antispasmodic drug, uncoated tablets, 40 mg

Two grades of uncoated tablets are investigated. Ten genuine tablets, subset N1, and 10 forgeries, subset N2. Twenty NIR spectra (3800–10,000 $cm^{-1}$, 1069 wavenumbers) were measured using the InAs detector. After that one tablet from set N1 was cut in half using a scalpel and a spectrum of the interior of a cut tablet was measured; this was named N1Cut. The same procedure was done for one tablet from set N2. As a result, in total 22 spectra were obtained. These spectra were pre-treated by MSC.

### 3.3. Data Set 3: antimicrobial drug, crushed tablets without coating

One of each of the grades of tablets used in Data Set 1 was crushed and imaged. The InGaAs imaging detector captured 86 images (256 × 320 pixels, 900–1750 nm, 10 nm intervals). The raw data was not corrected for dark or background signal. Dead pixels or hardware outliers were excluded from the PCA modeling.

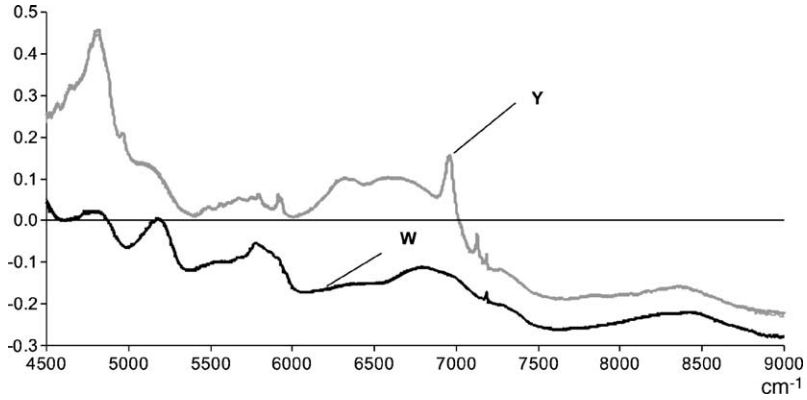


Fig. 1. MSC pre-treated spectra of Data Set 1. Black lines (W) are the W grade spectra and gray lines (Y) are the Y grade spectra.

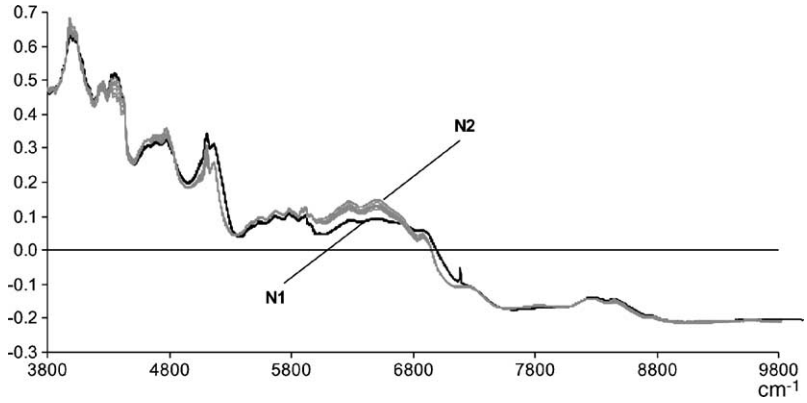


Fig. 2. MSC pre-treated spectra of Data Set 2. Black lines (N1) are 11 genuine tablets spectra and gray lines (N2) are 11 counterfeit tablets spectra.

## 4. Results and discussion

### 4.1. Data Set 1

The results of measurements of Data Set 1 after MSC pre-treatment (Fig. 1) show that these two grades of capsules have significantly different contents and the differences in their NIR-spectra are so obvious that no mathematical data processing is needed.

In cases where the counterfeit drugs have so manifest differences from the genuine drugs rather small sample sets and direct NIR-measurements are sufficient to discriminate between the grades.

### 4.2. Data Set 2

The results of measurements of Data Set 2 after MSC pre-treatment are shown in Fig. 2. Data pre-treatment is usually problem dependent. Centering NIR data before PCA analyses is a common place. As to scaling, we do not need such a transformation as this data are rather homogeneous, i.e. empirical variance is more-or-less comparable across the entire set of 1069 variable.

The data (22 samples and 1069 variables) are centered but not scaled and is subjected to a principal component analysis (Table 1, columns 1 and 2). Taking into account two principal components (PCs) we come to the following results (Fig. 3).

Table 1
PCA models for Data Set 2

| #PC, a | $N = 22$, $K = 1069$ | | $N = 22$, $K = 130$ | | $N = 10$, $K = 1069$ | | $N = 10$, $K = 130$ | |
|---|---|---|---|---|---|---|---|---|
| | $\lambda$ (1) | $\mu$ (2) | $\lambda$ (3) | $\mu$ (4) | $\lambda$ (5) | $\mu$ (6) | $\lambda$ (7) | $\mu$ (8) |
| 1 | 4.61 | 94.0 | 0.066 | 85.2 | 0.016 | 71.9 | 0.007 | 86.7 |
| 2 | 0.24 | 4.9 | 0.011 | 14.0 | 0.004 | 17.3 | 0.0009 | 10.4 |
| 3 | 0.041 | 0.8 | 0.0003 | 0.4 | 0.0002 | 6.1 | 0.0002 | 2.2 |
| 4 | 0.0007 | 0.1 | 0.0001 | 0.1 | 0.0001 | 3.8 | 0.0001 | 0.3 |

$\lambda$ is eigenvalue for corresponding PC, $\mu$ is the standardized eigenvalue.

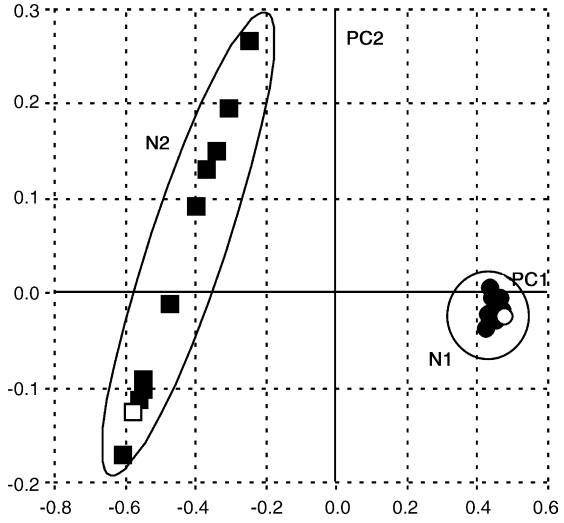


Fig. 3. PCA scores plot for Data Set 2. Dots represent genuine tablets (N1) and squares represent counterfeit tablets (N2). Open dots and squares show cut tablets.

Two manifest clusters in the PC1–PC2 plane are seen. Thus, the subsets N1 and N2 may easily be discriminated. The object variance in subset N2 (counterfeit drug) is significantly greater than the variance between objects in subset N1 (genuine tablets). This may be explained by better manufacturing control for genuine tablets. Spectra for the cut tablets are not different from the whole tablets (compare open dots and squares in Fig. 3 with closed ones) and have no influence on the results. Therefore, there is no need to cut such tablets for routine tests.

Form Fig. 2, the special regions where the difference between objects N1 and N2 is more evident could be found. These are the region (5800–6800 $cm^{-1}$) and a peak in the region (7000 and 7400 $cm^{-1}$) that is present in subset N1 and absent in spectra for N2 objects. These regions are shown in Fig. 4.

So, for the given data it is also possible to discriminate two groups without special mathematical processing, though the PCA score plot represents the information more clearly.

Now let us consider the initial narrow spectral region of wavelengths 3800–4300 $cm^{-1}$ (130 wavelengths), where it is impossible to separate groups N1 and N2 visually. But even in this case the PCA model with two components (Table 1, columns 3 and 4) shows a clear clustering on the score plot as presented in Fig. 5.

### 4.3. Pattern recognition for Data Set 2

In the previous section two groups of objects were discriminated: the genuine and the counterfeit tablets. But ordinarily there are several types of forgery tablets of the same drug. Taking into account that genuine tablets are rather similar to each other, the SIMCA method is applied to discriminate class N1 (genuine tablets) from *any other counterfeit tablets*. Ten objects from subset N1 (without cut tablet) are used to construct class N1. This is a rather small set of objects and only the first two PCs are used for modeling the common class properties (Table 1, columns 5–8). Two wavelength ranges are used for the PCA. The first range covers the whole NIR region, 1069 wavelengths (see Fig. 2), where two PCs explain 89% of the $X$ variance, and the second range covers the initial narrow region (see Fig. 5), where two PCs explain 91% of the $X$ variance.

To understand how far the new objects are to the model (class N1), the "membership plot" (Fig. 6) that presents the distance to model $s_i$ given by Eq. (2) versus leverage $h_i$ (Eq. (4)) can be used. The limits are shown as black lines: horizontal for the distance to model and vertical for the leverage. It may be easily seen from Fig. 6(a) that for the full spectra model the N1Cut object has a low leverage, but its distance to the model ($s_i$) is greater than the limit though it lies not far from the model. Samples from set N2 are very far from the

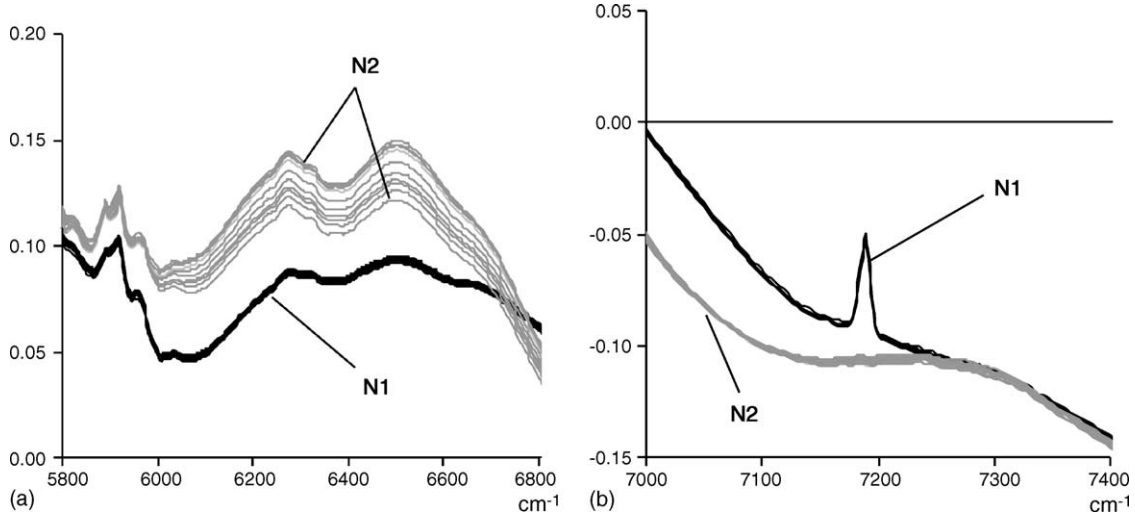


Fig. 4. Special regions in Data Set 2 spectra. Plots layout is similar to Fig. 2.

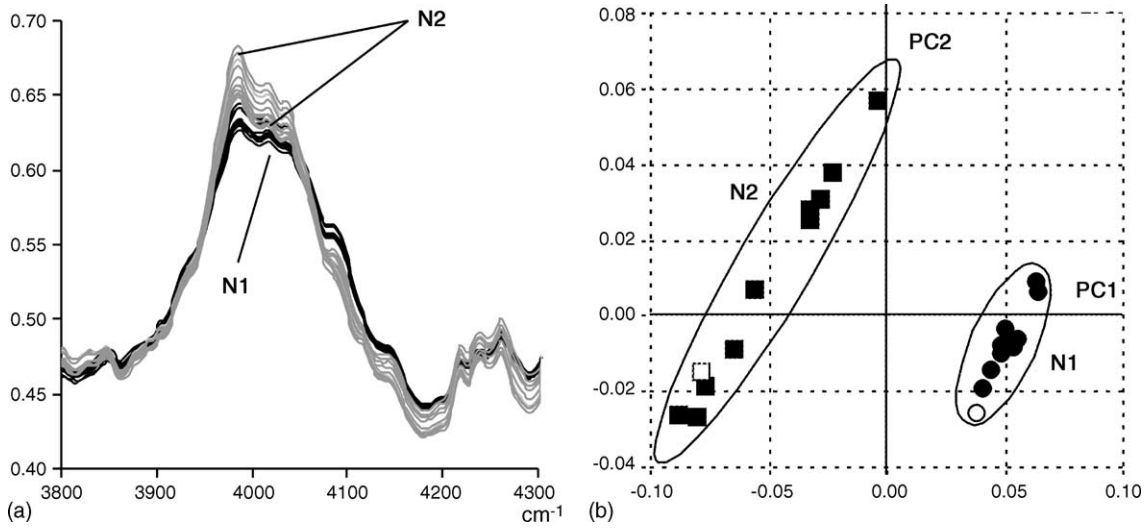


Fig. 5. PCA analysis of Data Set 2 based on narrow initial region of wavelengths: (a) narrow initial region of Data Set 2 spectra. Plot layout is similar to Fig. 2; (b) PCA score plot for narrow initial region. Plot layout is similar to Fig. 3.

model and undoubtedly can be classified as non-members of this class.

Classification based on the narrow spectral range is shown in Fig. 6(b). The results are similar to the previous model, with the only difference that the N1Cut sample is now classified as a member of the class of genuine tablets.

To build a general PCA model that describes the class of genuine samples of one type of drug it is necessary to collect a rather large and representative set of samples; samples produced at different times, samples with different shelf life, etc. Most likely it is not necessary to use all NIR spectral regions for model construction; this issue also can be determined only using a representative data set.

### 4.4. Data Set 3: image analysis

Multivariate image analysis (MIA) was performed on a subset of the entire image containing both tablet powders. The image hypercube is unfolded row by row, to create a large matrix of spectra for each pixel. Obvious dead pixel or outlier spectra are removed and the resulting matrix is mean centered and subjected to PCA. The first score vector is folded back to the original image dimensions to generate a score-image (Fig. 7(a)). A two-dimensional score plot is made of the first and third score vectors and color mapped to indicate the relative number of pixels at each score pair (Fig. 7(b)). Since the two-dimensional score plots are a projection from a higher dimension, different score vector pairings may accentuate different spectral features. The first and third score vectors were chosen to optimize the drug class separations. Clustering of points in this score plot can be attributed to the two tablet ingredients, image background, and the bottle cap containers. There are some scattering of score values due to shadow effects of the containers, surface irregularities in the powders, non-uniform lighting, and variation in the chemical composition of the tablet ingredients.

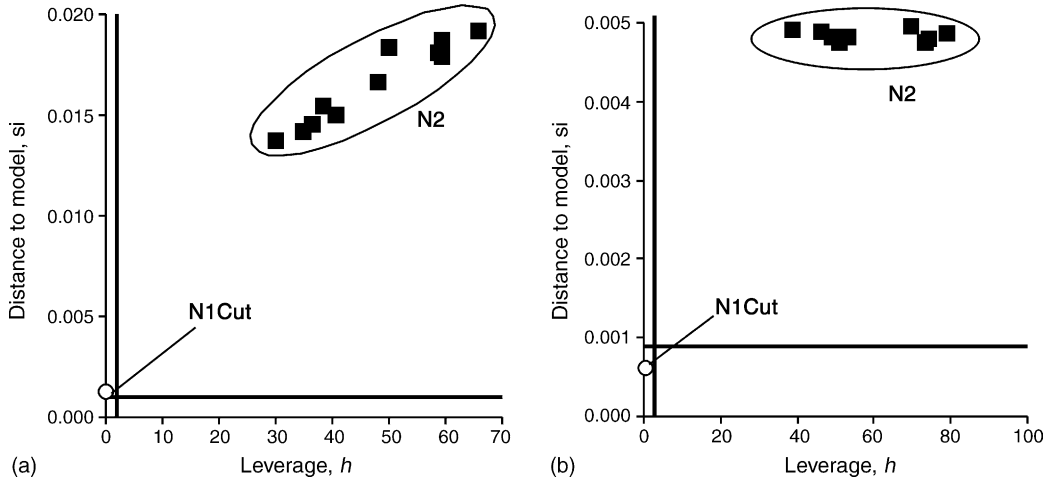


Fig. 6. SIMCA analysis of full and narrow spectra region of Data Set 2 for significance 0.05. Squares represent the counterfeit tablets (N2). Open dot (N1Cut) shows the cut genuine tablet: (a) full spectra; (b) narrow spectral region.

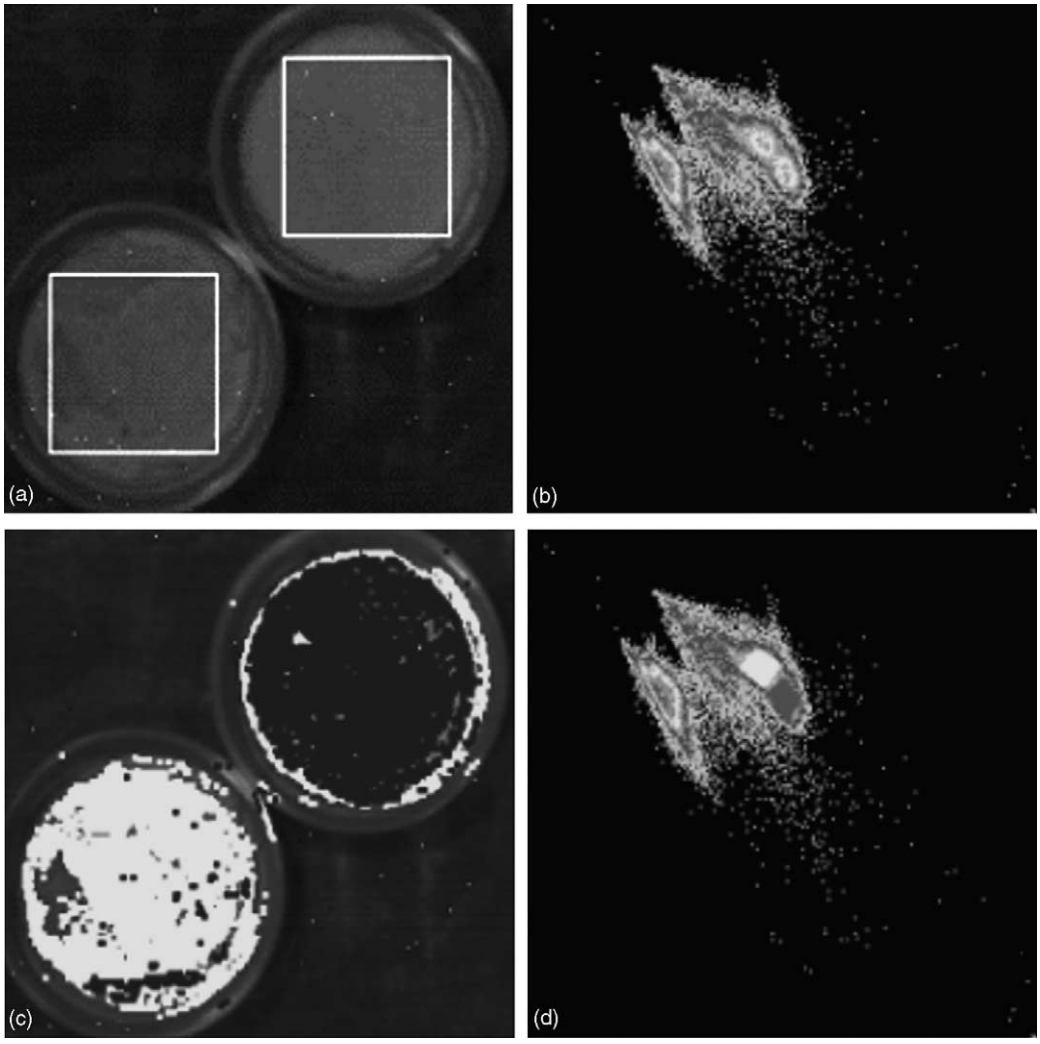


Fig. 7. Data Set 3. Multivariate image analysis: (a) T1 score image of crushed tablet ingredients; (b) T1–T3 score plot showing ingredient clustering; (c) class masks for two ingredients; (d) image mapping of pixels selected by masks.

Two distinct clusters can be seen which account for the two tablet ingredient classes "W" and "Y". Two polygon regions were created as class masks in the score plots (Fig. 7(d)). The sample spectra with points in these two regions are then mapped back into the original pixel coordinate system to indicate where they occur in the image (Fig. 7(c)). These two classes map almost completely into the two image regions of the two different tablet ingredients. There is a slight overlap or mixing of classes, however it must be noted that the two identified regions each contain nearly 7000 sample spectra or pixels. The class separation has been achieved.

Multivariate huperspectral image analysis provides additional diagnostic information. The first score image represents the maximum variation in the sample spectra, effectively summarizing what is different between image pixels and becomes a useful diagnostic tool for identifying non-homogeneous spatial regions of drug formulation. For example, individual whole tablets may be imaged and examined for distribution of active ingredients.

Interactive exploration of data between these two representations, the spatial or image display and the spectral rich score plots provides additional interpretation tools. Other score images may be created, or other score plots may be similarly mapped, but in this case the T1–T3 score plot showed the maximum separation of the two tablet pixel clusters.

### 4.5. Data Set 3: principle components analysis

Rectangles within the image are selected to represent the two tablet ingredient regions (Fig. 7(a)). PCA was performed on the mean centered spectra associated with the "W" tablet ingredient spectra. The "Y" tablet ingredient spectra were then centered and projected using this model. Fig. 8 shows the T1–T2 score plot of the entire 13,000 samples. The classes are not completely separated, however the median spectra from each class are statistically well separated. Non-uniform lighting, surface shadow effects and sample impurities contribute to overall variations in sample spectra and the variance

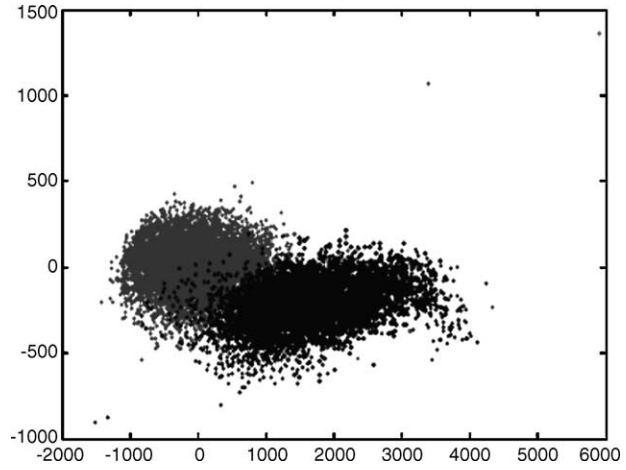


Fig. 8. Data Set 3. T1–T2 score plot of two class regions indicated in Fig. 7.

or distribution of points within each of the two classes of the score plot.

## 5. Conclusions

In general, there is one class of genuine drug samples and there may be plenty of forgeries of different degrees of similarity. Due to the production quality demands in the large pharmaceutical plants, the differences between the genuine items are rather small. Nevertheless, we consider this investigation as a feasibility study that yields promising results. For more trustworthy modeling it is necessary to collect a representative set of genuine samples of the drug produced at different times, with different shelf life, etc.

On the other hand, the diversity inside the counterfeit samples is essentially large. Sometimes the difference between the genuine and counterfeit drugs could be seen visually in the NIR spectra, but in other situations the answer is not so evident. To claim that a sample is a forgery, it is not necessary to compare the concentrations of active ingredients. All that is needed is to check whether a given sample is identical to the genuine drug or not. The above analysis shows that the NIR approach together with PCA has good prospects and may efficiently substitute wet chemistry.

The lower spectral resolution of the NIR camera may appear to contribute to the loss of information and class discrimination. However, the very large numbers of samples makes it possible to compute population statistics and routinely discard problematic sample spectra. MIA will be important for future studies where bulk/point analysis is unable to detect differences. Even in cases where bulk analysis can detect small differences, image analysis will be able to corroborate the findings by giving further information. Adding the ability to examine spatial location of spectral characteristics makes multivariate hyperspectral image analysis a powerful tool in examination of drug forgeries.

## 6. Software

All calculations for NIR data (pre-treatment, PCA, SIMCA) were made using The Unscrambler 8.0 software [22]. The hyperspectral image exploratory work was done with a multivariate image analysis tool JIMIA, written in Java (by J. Burger), calibration and chemometric routines were coded in MATLAB.

## References

[1] WHO, Counterfeit Drugs: Guidelines for the Development of Measures to Combat Counterfeit Drugs, WHO, Geneva, 1999.
[2] FIP Statement of Policy on Counterfeit Medicines, Int. Pharmacy J. 17-2 (2003) 11–12.
[3] World Health Assembly, Counterfeit drugs: Threat to Public Health, vol. 55, World Health Assembly, Geneva, 2002.
[4] A.S. Kenyon, T.P.A. Layoff, Compendium of Unofficial Methods for Rapid Screening of Pharmaceuticals by Thin-layer Chromatography, FDA, St. Louis, MO, 1999.
[5] A.S. Kenyon, Rapid Screening of TB Pharmaceuticals by Thin-layer Chromatography, FDA, St. Louis, MO, 1999.
[6] WHO, Basic Tests for Pharmaceutical Substances, WHO, Geneva, 1986.
[7] WHO, Basic Tests for Drugs, WHO, Geneva, 1998.
[8] WHO, Basic Tests for Pharmaceutical Dosage Forms, WHO, Geneva, 1991.
[9] A.P. Arzamastsev, V.L. Dorofeyev, V.Yu. Kochin, et al. Using Thin-Layer Chromatography for the Fast Identification of the Fluoroquinolone Drugs. World Congress of Pharmacy and Pharmaceutical Sciences 2002: 62nd International Congress of FIP, Nice, p. 39.
[10] A.P. Arzamastsev, V.L. Dorofeyev, et al. Express-analysis for the Detection of Counterfeit Drugs. Manual, Fluoroquinolones and Cephalosporines, 2003 (in Russian).
[11] A.P. Arzamastsev, V.L. Dorofeev, A.A. Konovalov, V.Yu. Kochin, I.V. Titov, Determining adulterated drugs by modern analytical techniques, Pharm. Chem. J. 38 (2004) 166–169.
[12] W. Wu, B. Walczak, D.L. Massart, S. Heuerding, F. Erni, I.R. Last, K.A. Prebble, Artificial neural networks in classification of NIR spectral data: design of the training set, Chemomet. Intell. Lab. Syst. 33 (1996) 35–46.
[13] J. Sjoblom, O. Svensson, M. Josefson, H. Kullberg, S. Wold, An evaluation of orthogonal signal correction applied to calibration transfer of near infrared spectra, Chemomet. Intell. Lab. Syst. 44 (1998) 229–244.
[14] N.-O. Lindberg, J. Gabrielsson, Use of software to facilitate pharmaceutical formulation–experiences from a tablet formulation, J. Chemomet. 18 (2003) 133–138.
[15] T. Næs, T. Isaksson, T. Fearn, T. Davies, Multivariate Calibration and Classification, NIR Publications, 2002.
[16] J. Gabrielson, N.-O. Lindberg, T. Lundstedt, Multivariate methods in pharmaceutical applications, Rev. J. Chemomet. 16 (2002) 141–160.
[17] S. Wold, K. Esbensen, P. Geladi, Principal component analysis, Chemomet. Intell. Lab. Syst. 2 (1987) 37–52.
[18] H. Martens, T. Naes, Multivariate Calibration, Wiley, New York, 1998.
[19] S. Wold, Pattern recognition by means of disjoint principal components models, Pattern Recogn. 8 (1976) 127–139.
[20] P. Geladi, H. Grahn, Multivariate Image Analysis, Wiley, Chichester, 1996.
[21] K.H. Esbensen, Multivariate Data Analysis – In Practice, 4th ed., CAMO, 2000.
[22] The Unscrambler's User's Guide, Version 8.0, Camo, Trondheim, 2004.